coatings

MDPI

Article

Preparation of Chitosan-Modified Nano-Silver Solution Microcapsules and Their Effects on Antibacterial Properties of Waterborne Coatings

Ying Wang [1,2], Pan Pan [1,2] and Xiaoxing Yan [1,2,*]

[1] Co-Innovation Center of Efficient Processing and Utilization of Forest Resources, Nanjing Forestry University, Nanjing 210037, China; wangying1214@njfu.edu.cn (Y.W.); pan@njfu.edu.cn (P.P.)
[2] College of Furnishings and Industrial Design, Nanjing Forestry University, Nanjing 210037, China
* Correspondence: yanxiaoxing@njfu.edu.cn

Abstract: In this paper, a chitosan-modified nano-silver solution was used as the core material of an antibacterial agent, and melamine formaldehyde resin was coated onto the core material to obtain the antibacterial microcapsules. The core/wall ratio, the stirring rate, the mass ratio of chitosan to silver ions, and the concentration of the emulsifier were used to carry out four-factor and three-level orthogonal experiments to explore the most significant factors affecting the coverage rate and output of microcapsules and the best preparation technology. The results showed that the concentration of the emulsifier was the most important factor affecting the preparation of microcapsules. The higher the concentration of the emulsifier, the better the dispersed morphology of microcapsules, and the higher the coverage rate, up to 44.0%. The antibacterial coating was prepared by mixing microcapsules with a waterborne primer at a content of 4.0%. Its optical properties, mechanical properties, and antibacterial properties were analyzed. By increasing the concentration of the emulsifier, the gloss of the coating showed a trend of first increasing and then decreasing. When the emulsifier concentration was 2.0%, the gloss of the Andoung wood surface coating reached the maximum value of 21.23%. The influence of emulsifier concentration on the color difference of coating had no obvious law, and it was negatively related to the light transmittance. In terms of mechanical properties, the concentration of the emulsifier is directly proportional to the hardness and impact resistance of the coating, with the maximum reaching 31 kg·cm, and is negatively related to adhesion and roughness. In terms of antibacterial properties, the higher the concentration of the emulsifier, the better the antibacterial properties of the coating. When the concentration of the emulsifier was 4.0%, the antibacterial rates of coating which coated the glass substrate were 71.3% and 80.0% for *Escherichia coli* and *Staphylococcus aureus*, respectively. The antibacterial rates of the Andoung wood surface coating reached the maximum, which were 68.4% and 73.2%, respectively, and the antibacterial performance was excellent. In this study, an efficient antibacterial microcapsule for waterborne coatings was prepared, which provided the reference value for the application of antibacterial microcapsules in waterborne coatings.

Keywords: microcapsule; antibacterial; emulsifier concentration; mechanical property

Citation: Wang, Y.; Pan, P.; Yan, X. Preparation of Chitosan-Modified Nano-Silver Solution Microcapsules and Their Effects on Antibacterial Properties of Waterborne Coatings. *Coatings* **2023**, *13*, 1433. https://doi.org/10.3390/coatings13081433

Academic Editors: Gabriela Olimpia Isopencu, Ajay Vikram Singh and Alexandra Mocanu

Received: 30 June 2023
Revised: 28 July 2023
Accepted: 4 August 2023
Published: 15 August 2023

1. Introduction

Wood is an important component material for furniture products and has always been favored [1–4]. However, the lignin, cellulose, hemicellulose, and other components in wood easily degrade to water, carbon dioxide, and glucose, resulting in wood materials suffering from pests, pathogens, bacteria, and other microbial invasions [5–8]. The wood insects, mold, mildew, etc. [9,10], not only shorten the service life of wood, but also limit its application [11,12]. Coating treatment is an effective antibacterial method on the surface of wood substrates and has special functions of resistance to corrosion, heat, water, and fire, to protect and beautify the surface of wood, close the wood pipe hole,

and improve the utilization of wood stability [13]. Waterborne coating uses water as a diluent, does not contain organic solvents, and exhibits excellent performance such as environmental protection and safety [14], so it is possible to add antibacterial agents directly into waterborne coatings to deactivate or destroy the reproduction ability of bacteria and microorganisms, and achieve antibacterial effects without changing the structure of the wood itself [15].

In the engineering and biomedical fields, nanostructures have attracted attention because of their biocompatibility and negligible cytotoxicity. Ehsan et al. [16] summarized the green synthesis of non-spherical metal/metal oxide and carbon-based nanoarchitectures, and their activities for biomedical applications. Matineh et al. [17] studied the functionalized polymer and nanomaterial surfaces with antimicrobial therapy and drug delivery. Silver-based antibacterial materials mainly include silver ions and nano-silver. The silver ions can be adsorbed on the surface of bacteria to deactivate DNA, enzymes, proteins, etc. [18,19]. Nano-silver is a silver monolith generated using physicochemical methods, with a small size of nanomaterials, uniform distribution, large specific surface area, nontoxic environmental protection, and other stable characteristics [20–23]. Francis et al. [24] utilized a filamentous fungus (*Sclerotium rolfsii*) as a soft bio-template to generate silver nanoparticle (AgNP) microtubules adhering to the fungal hyphae. The resulting composite exhibited antibacterial properties against *Staphylococcus aureus* and *Escherichia coli* bacteria. Pan et al. [25] prepared antibacterial nano-silver solution microcapsules, and their effect on the properties of a wood surface coating was investigated. Silver-based antimicrobial materials have broad-spectrum antibacterial properties, but due to their high active surface area and easy oxidation, nano-silver is prone to aggregation and deactivation, thus reducing its antimicrobial effect [26]. Pakpoom et al. [27] blended AgNP colloids with chitooligomers and monomers (COAMs) to create the composites and verified the synergistic antibacterial effects of AgNPs–COAMs. Omnia et al. [28] prepared a new epoxy/chitosan–Ag nanocomposite coating and found that Ag and chitosan nanoparticles can improve the anticorrosion ability. The new nanocomposite was used as an anticorrosion coating for steel in a sodium chloride solution. In order to achieve a long-lasting antibacterial effect, a chitosan–silver composite antibacterial agent was synthesized by the complexation of silver ions and chitosan. The purpose is to improve the stability and antibacterial properties of the composite antibacterial agent. The chitosan molecule contains amino side groups. The ortho of -NH_2 is -OH, which can form a cage molecule with a similar net-like structure through hydrogen bonding and also through salt bonding, to make the chitosan molecule exert a stable coordination effect on metal ions [29]. The antibacterial property of chitosan comes from the protonated amino group on C_2 in the molecular structure of chitosan [30]. The chitosan powder itself does not have antibacterial properties and needs to be dissolved in acidic conditions in order to exert antibacterial properties. However, in a neutral or alkaline environment, the antibacterial property of chitosan is greatly reduced due to the reduction in protonated amino groups. Therefore, compounding Ag^+ with chitosan can not only improve the antibacterial property of chitosan, but also make Ag^+ well immobilized or adsorbed, so that the two can play complementary roles. The use of microencapsulation technology to encapsulate the core-material antibacterial agent can provide various excellent advantages such as controlled release and isolation [31–34]. The application of antibacterial microcapsules to waterborne coatings on wood surfaces is simple and convenient, using coating technology without changing the shape and structure of the wood, and without losing the performance of the original substrate. The wood surface can be quickly implemented to prepare an antibacterial functional waterborne coating, which has important practical significance for improving the service life of the coating, for long-lasting antibacterial properties, and for protecting the substrate.

In this paper, the chitosan-modified nano-silver solution was used as the core material, and the melamine–formaldehyde (MF) resin was used to cover the core material to obtain the antibacterial microcapsules. Orthogonal experiments were used to investigate the best preparation process of microcapsules. The microcapsules were added to a waterborne

coating to prepare an antibacterial coating. The antibacterial coating was applied to the surface of wood. The physical and chemical properties of the coating were studied by optical and mechanical tests, and the antibacterial properties of the coating were studied using the dilution coating plate counting method.

2. Materials and Methods

2.1. Materials of Test

The materials needed in the test have been listed as shown in Table 1. The glass substrate is made of pathology-grade slide, the material is float glass, the model is 7101P-G, and the specification is 25 mm × 75 mm, provided by Jiangsu Nantong Hairui Co., Ltd., Nantong, China. The Andoung wood (*Monopetalanthus* spp.) is provided by the laboratory with the specification of 50 mm × 100 mm × 5 mm, which has been polished smoothly. The molecular weight of chitosan is 160.9, and the degree of deacetylation is 80.0%–95.0%. The silver ion content of nano-silver solution is 25 PPM, the particle size is 5–7 nm, the pH value is 3–5, and the density is 1.2 g/cm^3. The waterborne coating is Dulux waterborne primer. *Escherichia coli* is the second-generation standard strain ATCC25922, and *Staphylococcus aureus* is the second-generation standard strain ACTT6538.

Table 1. List of experimental material information.

Material	Specification	Manufacturer
37.0% Formaldehyde	analytically pure	Nantong Yaoxin Chemical Co., Ltd., Nantong, China
Melamine	analytically pure	Shandong Yousuo Chemical Industry Technology Co., Ltd., Shandong, China
Triethanolamine	analytically pure	Shanxi Panlong Yihai Pharmaceutical Co., Ltd., Xi'an, China
Span-80	analytically pure	Wuxi Yatai United Chemical Co., Ltd., Wuxi, China
Nano-silver solution	analytically pure	Tianjin Beichen Founder Reagent Factory, Tianjin, China
Chitosan	analytically pure	Shanghai National Medicine Reagent Co., Ltd., Shanghai, China
Citric acid monohydrate	analytically pure	Nanjing Quanlong Biotechnology Co., Ltd., Nanjing, China
Absolute ethanol	analytically pure	Guangzhou Kema Chemical Technology Co., Ltd., Guangzhou, China
Ethyl acetate	analytically pure	Xi'an Tianmao Chemical Co., Ltd., Xi'an, China
Acetic acid	analytically pure	Shanghai National Medicine Reagent Co., Ltd., Shanghai, China
Waterborne coating	analytically pure	Akzo Nobel Paint Co., Ltd., Guangzhou, China
Escherichia coli	-	Beijing Conservation Biotechnology Co., Ltd., Beijing, China
Staphylococcus aureus	-	Beijing Conservation Biotechnology Co., Ltd., Beijing, China
Nutrient broth	-	Hangzhou Chicheng Pharmaceutical Technology Co., Ltd., Hangzhou, China
Eluent	-	Sichuan Kelun Pharmaceutical Co., Ltd., Chengdu, China

2.2. Preparation of Chitosan-Modified Nano-silver Solution

Dissolution of chitosan: A total volume of 30 mL acetic acid solution with a concentration of 1.0% was prepared for use. An amount of 0.36 g of chitosan powder was added into the acetic acid solution to dissolve, and then the pH value was adjusted to 5 with 0.5 mol/L NaOH. At a water bath temperature of 30 °C, the prepared solution was stirred with a magnetic stirring rotor for 30 min to obtain a clear, transparent, and thick chitosan solution.

Preparation of chitosan-modified nano-silver solution: According to the best mass ratio, a certain amount of nano-silver solution was directly dropped into the completely dissolved chitosan solution, and the chitosan-modified nano-silver solution was obtained after sufficient stirring.

2.3. Preparation of Chitosan-Modified Nano-Silver Solution Microcapsules

Preparation of wall material: An amount of 7.29 g of 37% formaldehyde, 36.45 mL of distilled water, and 14.52 g of melamine were added to the beaker with a molar ratio of formaldehyde to melamine of 1:3. Triethanolamine was added dropwise to adjust the pH value to 8–9, the water bath temperature was 70 °C, the stirred speed was 600 rpm, and the reaction time was 30 min. Finally, the MF prepolymer was obtained.

Preparation of core material: An amount of 0.50 g Span-80 and 49.50 mL ethanol were mixed to obtain a concentration of 1% Span-80 emulsifier. The chitosan-modified nano-silver solution was added dropwise in the beaker through a pipette. At water bath temperature of 60 °C, the mixed solution was stirred for 1 h.

Preparation of chitosan-modified nano-silver solution microcapsules: The MF prepolymer was added into the core emulsion slowly drop by drop at a certain speed. The pH value was adjusted with citric acid monohydrate at a certain speed. When the pH value reached 3.5−5.0, the water bath temperature was 60 °C, and the mixture reacted at a constant temperature for 3 h. After 3 days, the product was repeatedly rinsed and filtered with anhydrous ethanol until the filtered liquid was clear, and then it was placed in an oven at 60 °C to dry to obtain the microcapsules.

Four-factor and three-level orthogonal experiments were then designed, and the major factors affecting the preparation of microcapsules were screened. The factors and levels of orthogonal experiments are shown in Table 2. The orthogonal test plan is shown in Table 3. "#" is a sample number unit. The specific amounts of substances in orthogonal experiments are shown in Table 4. A detailed list of substances used in the single-factor test is shown in Table 5.

Table 2. Orthogonal test factors and levels.

Level	W_{core}/W_{wall}	$W_{chitosan}/W_{silver\ ion}$	Emulsifier Concentration (%)	Rotational Speed (rpm)
1	0.75:1	500:1	1	400
2	0.80:1	1000:1	2	600
3	0.85:1	2000:1	3	800

Table 3. Orthogonal test schedule.

Sample (#)	W_{core}/W_{wall}	$W_{chitosan}/W_{silver\ ion}$	Emulsifier Concentration (%)	Rotational Speed (rpm)
1	0.75:1	500:1	1	400
2	0.75:1	1000:1	2	600
3	0.75:1	2000:1	3	800
4	0.80:1	500:1	2	800
5	0.80:1	1000:1	3	400
6	0.80:1	2000:1	1	600
7	0.85:1	500:1	3	800
8	0.85:1	1000:1	1	600
9	0.85:1	2000:1	2	400

Table 4. Detailed list of substances used in orthogonal test.

Sample (#)	Melamine (g)	37.0% Formaldehyde (g)	Deionized Water (g)	Nano-silver Solution (g)	Chitosan (g)	Acetic Acid (mL)	Span-80 (g)	Absolute Ethanol (g)	Rotational Speed (rpm)
1	7.08	14.10	35.38	9	0.09	20	0.8	79.20	400
2	7.15	14.24	35.73	9	0.18	25	1.2	58.80	600
3	7.29	14.52	36.43	9	0.36	30	1.6	53.30	800
4	6.63	13.22	33.17	9	0.09	25	1.2	58.80	800
5	6.70	13.35	33.50	9	0.18	30	1.6	53.30	400
6	6.83	13.61	34.16	9	0.36	20	0.8	79.20	600
7	6.24	12.44	31.22	9	0.09	30	1.6	53.30	800
8	6.31	12.57	31.53	9	0.18	20	0.8	79.20	600
9	6.43	12.81	32.15	9	0.36	25	1.2	58.80	400

Table 5. Detailed list of substances used in single-factor test.

Sample (#)	Melamine (g)	37.0% Formaldehyde (g)	Deionized Water (g)	Nano-silver Solution (g)	Chitosan (g)	Acetic Acid (mL)	Span-80 (g)	Absolute Ethanol (g)	Rotational Speed (rpm)
10	7.29	14.52	36.45	9	0.36	30	0.25	49.75	800
11	7.29	14.52	36.45	9	0.36	30	0.50	49.50	800
12	7.29	14.52	36.45	9	0.36	30	0.75	49.25	800
13	7.29	14.52	36.45	9	0.36	30	1.00	49.00	800
14	7.29	14.52	36.45	9	0.36	30	1.25	48.75	800
15	7.29	14.52	36.45	9	0.36	30	1.50	48.50	800
16	7.29	14.52	36.45	9	0.36	30	2.00	48.00	800
17	7.29	14.52	36.45	9	0.36	30	2.50	47.50	800

2.4. Preparation of Antibacterial Coating

The substrates chosen for the experiments were glass plates and the Andoung wood, respectively. The 8 groups of antibacterial microcapsules in the single-factor test were mixed with the waterborne primer at 4.0% microcapsule content. The microcapsules and waterborne primer were weighed at a total of 4 g. The coating process included 2 coats of primer. The sample was primed once and then dried in an oven at 60 °C for 30 min, and the surface of the coating was sanded with 800 # sandpaper before the second coat. Then, the second layer of primer was coated and cured under the same process to conduct relevant tests.

2.5. Testing and Characterization

2.5.1. Testing and Characterization of Microcapsules

(1) Output and coverage rate: The mass of microcapsule powder after drying is the output, and the unit is g. An amount of 1 g of microcapsules (M_1) was weighed, fully ground in a mortar, soaked in ethyl acetate for 48 h, and then in ethanol for 24 h. The remaining materials were repeatedly rinsed with deionized water until the filtered solution was clear and free of air bubbles, and the remaining materials were weighed after drying (M_2). The coverage rate (C) was calculated by Equation (1):

$$C = (M_1 - M_2)/M_1 \times 100\% \quad (1)$$

(2) Microstructure analysis: The microstructures of microcapsules and coatings were observed using a Zeiss Axio Scope A1 optical microscope (OM, Carl Zeiss, Oberkohen, Germany) and a Zeiss Sigma 300 scanning electron microscope (SEM, FEI Company, Hillsboro, OR, USA). The SEM images of microcapsules were also analyzed for particle size using Nano Measurer software with a particle size sample measurement capacity of 100.

(3) Infrared spectrum analysis: A VERTEX 80 V infrared spectrometer (FTIR, Bruker GmbH, Karlsruhe, Germany) was used for the analysis of the chemical composition of microcapsules and coatings in the range 4000–500 cm^{-1} with a resolution of 4 cm^{-1}.

(4) Formaldehyde emission test: A model DM105D air quality detector (Landeley Technology Co., Ltd., Shenzhen, China) was used for the formaldehyde emission test.

2.5.2. Performance Characterization of Antibacterial Coating

(1) Color difference: According to GB/T 11186.3-1989 [35], an SEGT-J color difference meter (Suzhou Weifu Photoelectric Technology Co., Ltd., Suzhou, China) was used to measure the chromaticity value. The color difference value (ΔE) is as Formula (2):

$$\Delta E = [(\Delta L^*)^2 + (\Delta a^*)^2 + (\Delta b^*)^2]^{1/2} \quad (2)$$

(2) Gloss: According to GB/T 9754-2007 [36], the gloss of coating was measured by an HG268 intelligent gloss meter (Shenzhen Linshang Technology Co., Ltd., Shenzhen, China).

(3) Coating transmittance: Using a U-3900 HITACHI type UV spectrophotometer (Shanghai Smeo Analytical Instrument Co., Ltd., Shanghai, China), the transmittance value of the coating applied to the glass substrate was measured in the range of 300−800 nm.

(4) Hardness: According to GB/T 6739-2006 [37], 6H–6B pencils (Shenzhen Forest Precision Instrument Co., Ltd., Guangzhou, China) were selected to measure the hardness of the coating. The tested pencils were used under a 1.0 kg load at a scratch angle of 45°.

(5) Impact resistance: According to GB/T 4893.9-2013 [38], a QCJ-50 coating film impact tester (Shenzhen sanuo Experimental Equipment Co., Ltd., Shenzhen, China) was selected to test the impact resistance of the coating. A 1.0 kg hammer was released to produce impact on the coating, using a 4-times magnification glass to judge whether the coating has cracks, wrinkles, peeling, etc. The maximum strength that did not cause damage to the coating was recorded as impact resistance.

(6) Adhesion: According to GB/T 4893.4-2013 [39], a QFH-HG600 film scriber (Hebei Zhongke Beigong Test Instrument Co., Ltd., Cangzhou, China) was selected to test the

adhesion of the coating. The adhesion level decreased from 0 to 5. The surface of the coating did not peel off when the grade was 0.

(7) Roughness: A JB-4C precision roughness meter (Shanghai Taiming Optical Instrument Co., Ltd., Shanghai, China) was used to determine the roughness of the coating, using the needle tracing method and selecting the places on the main surface of the coating. Subsequently, according to the measurement results of each place, the roughness of the coating was evaluated comprehensively. The unit of roughness is μm.

2.5.3. Testing and Characterization of Antibacterial Properties of Coating

(1) Strain preservation: The *Escherichia coli* and *Staphylococcus aureus* slant media were placed at 0−5 °C for preservation.

(2) Strain activation: The required strains were inoculated onto the plate nutrient agar medium at the temperature of 36−38 °C, and were cultivated for 18−20 h. A small number of fresh bacteria were scraped from the inoculated medium with an inoculating ring and added to the broth to culture. The concentration of the culture solution required for the experiment is (5.0−10.0) × 10^5 cfu/mL (total number of bacterial communities contained in the sample) of the broth.

(3) Sample test: A pipette was used to take 0.4−0.5 mL of test bacterial solution to add drop by drop on blank control sample plate and antibacterial coating sample plate, respectively. A plastic film was sterilized for use. The sample plates were covered with the plastic film, making sure there were no air bubbles. The plastic film was gently pressed down to make the suspension spread around to make the strain evenly touch the sample. Then, the sample was transferred to a constant temperature and humidity chamber for 24 h, with the temperature of 38 °C and relative humidity >90%.

(4) Dilution coating plate method to prepare agar plate: A volume of 20 mL of eluent was used to repeatedly rinse the coating and plastic film. The washing solution was added to the agar medium. When the agar was solidified, bacteria-containing agar plates were obtained. The colony was obtained after 48 h of cultivation at 38 °C. Finally, the number of bacteria was counted with a colony counter, and the results of the viable bacteria measured above were multiplied by 1000 to obtain an actual recovery bacteria value after culturing for 24 h. The unit is CFU/mL. The calculation formula is as Formula (3) [40]:

$$R = (B - C)/B*100\% \quad (3)$$

R = Antibacterial rate, expressed in %;

B = Actual recovery bacteria value after culturing for 24h for blank control sample;

C = Actual recovery bacteria value after culturing for 24h for antibacterial coating sample.

The error of all experiments was controlled within 5% and repeated four times.

3. Results and Discussion

3.1. Analysis of Output and Coverage of Microcapsules in Orthogonal Tests

The output is an important reference to measure the results of microcapsule preparation, and it is of great importance to obtain high output with a small amount of raw material in the actual production process. As shown in Table 6, according to the range results, it is concluded that the main factor affecting the output of microcapsules is the emulsifier concentration. The better process parameters for the preparation of microcapsules based on the range results are: W_{core}/W_{wall} is 0.75:1, $W_{chitosan}/W_{silver\ ion}$ is 2000:1, the rotational speed is 800 rpm, and the concentration of emulsifier is 2.0%.

Table 6. Range and significance results based on output.

Sample (#)	W_{core}/W_{wall}	$W_{chitosan}/W_{silver\ ion}$	Emulsifier Concentration (%)	Rotational Speed (rpm)	Output (g)
1	0.75:1	500:1	1	400	8.8
2	0.75:1	1000:1	2	600	11.05
3	0.75:1	2000:1	3	800	12.55
4	0.80:1	500:1	2	800	11.13
5	0.80:1	1000:1	3	400	9.00
6	0.80:1	2000:1	1	600	9.44
7	0.85:1	500:1	3	600	8.31
8	0.85:1	1000:1	1	800	9.24
9	0.85:1	2000:1	2	400	10.46
Mean 1	10.800	9.413	9.160	9.420	-
Mean 2	9.857	9.763	10.880	9.600	-
Mean 3	9.337	10.817	9.953	10.973	-
Range	1.463	1.404	1.720	1.553	-
Sum of Squared Deviations	3.302	3.302	4.446	4.331	15.28
Degrees of Freedom	2	2	2	2	8
F_{ratio}	0.864	0.838	1.164	1.134	-
$F_{critical}$ Value	4.460	4.460	4.460	4.460	-
Significance	-	-	-	-	-

The coverage rate is the key to evaluate the success of microcapsule encapsulation and also affects the antibacterial properties of microcapsules. As shown in Table 7, the variance results showed that the important factor affecting the coverage rate of microcapsules was the emulsifier concentration. From the range results, it can be seen that the better process parameters for the preparation of microcapsules are: W_{core}/W_{wall} is 0.75:1, $W_{chitosan}/W_{silver\ ion}$ is 2000:1, the emulsifier concentration is 1.0%, and stirring speed is 800 rpm.

Table 7. Range and significance results based on coverage rate.

Sample (#)	W_{core}/W_{wall}	$W_{chitosan}/W_{silver\ ion}$	Emulsifier Concentration (%)	Rotational Speed (rpm)	Coverage Rate (%)
1	0.75:1	500:1	1	400	45
2	0.75:1	1000:1	2	600	44
3	0.75:1	2000:1	3	800	45
4	0.80:1	500:1	2	800	41
5	0.80:1	1000:1	3	400	41
6	0.80:1	2000:1	1	600	45
7	0.85:1	500:1	3	600	40
8	0.85:1	1000:1	1	800	44
9	0.85:1	2000:1	2	400	43
Mean 1	34.667	32.000	34.667	33.000	-
Mean 2	32.333	33.000	32.667	33.000	-
Mean 3	32.333	34.333	32.000	33.333	-
Range	2.334	2.333	2.667	0.333	-
Sum of Squared Deviations	10.889	8.222	11.556	0.222	30.89
Degrees of Freedom	2	2	2	2	8
F_{ratio}	1.410	1.065	1.496	0.029	-
$F_{critical}$ Value	4.460	4.460	4.460	4.460	-
Significance	-	-	-	-	-

As shown in Figure 1, the core-to-wall ratio is inversely correlated with the output of microcapsules, the larger the mass ratio of chitosan to silver ions, the higher the output of microcapsules. As the emulsifier concentration increased, the output of microcapsules first increased and subsequently dropped. The faster the stirring speed, the higher the output. As shown in Figure 2, the higher the concentration of emulsifier, the worse the coverage rate. The mass ratio of chitosan to silver ions was positively correlated with the coverage rate of the microcapsule; the faster the stirring speed, the higher the coverage rate. The larger the mass ratio of chitosan to silver ions, the higher the coverage rate of microcapsules. The orthogonal test results showed that the emulsifier concentration was the most important factor affecting the output and coverage rate of microcapsules. In order to obtain the best process for the preparation of antibacterial microcapsules, the single-factor experiments were designed with the emulsifier concentration as the variable and the other three parameters fixed.

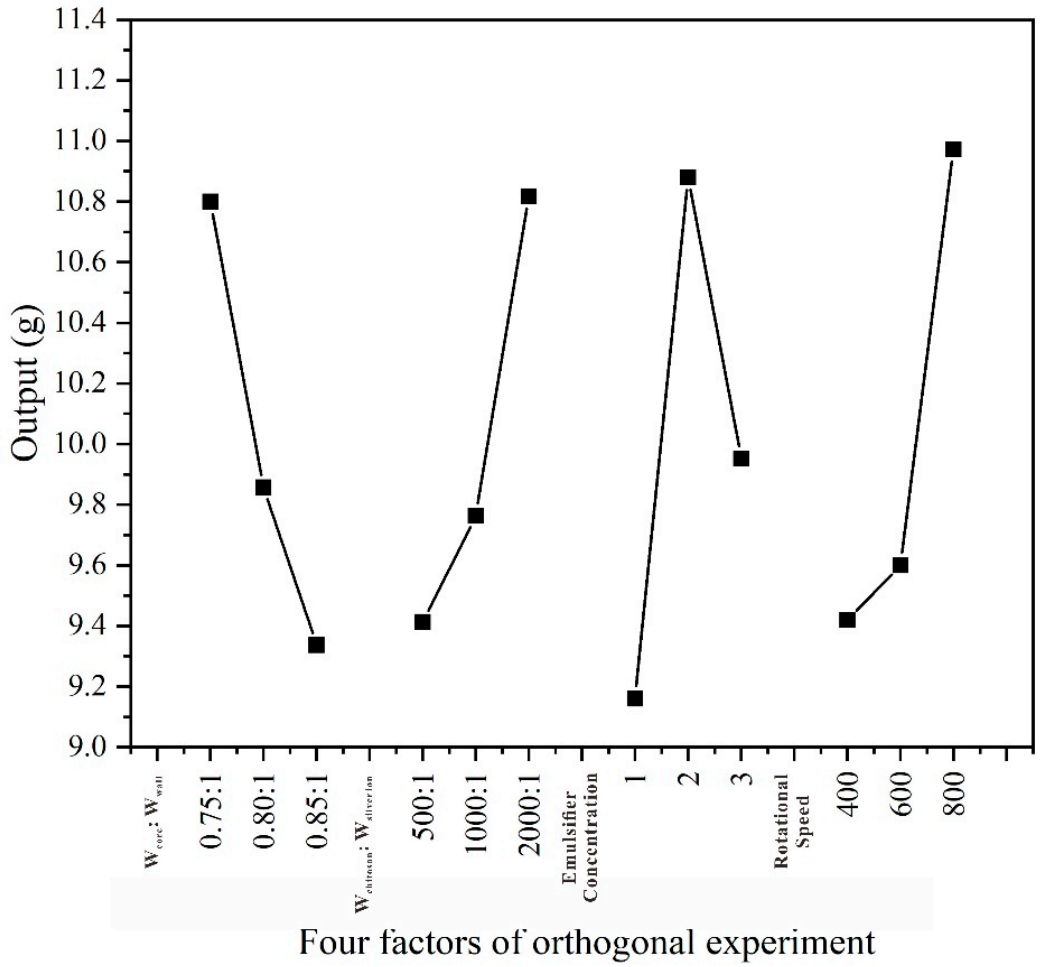

Figure 1. Effect curve of orthogonal experiment factors on output. The first line is effect of W_{core}/W_{wall} on output, the second line is effect of $W_{chitosan}/W_{silver\ ion}$ on output, the third line is effect of emulsifier concentration on output, the fourth line is effect of rotational speed on output.

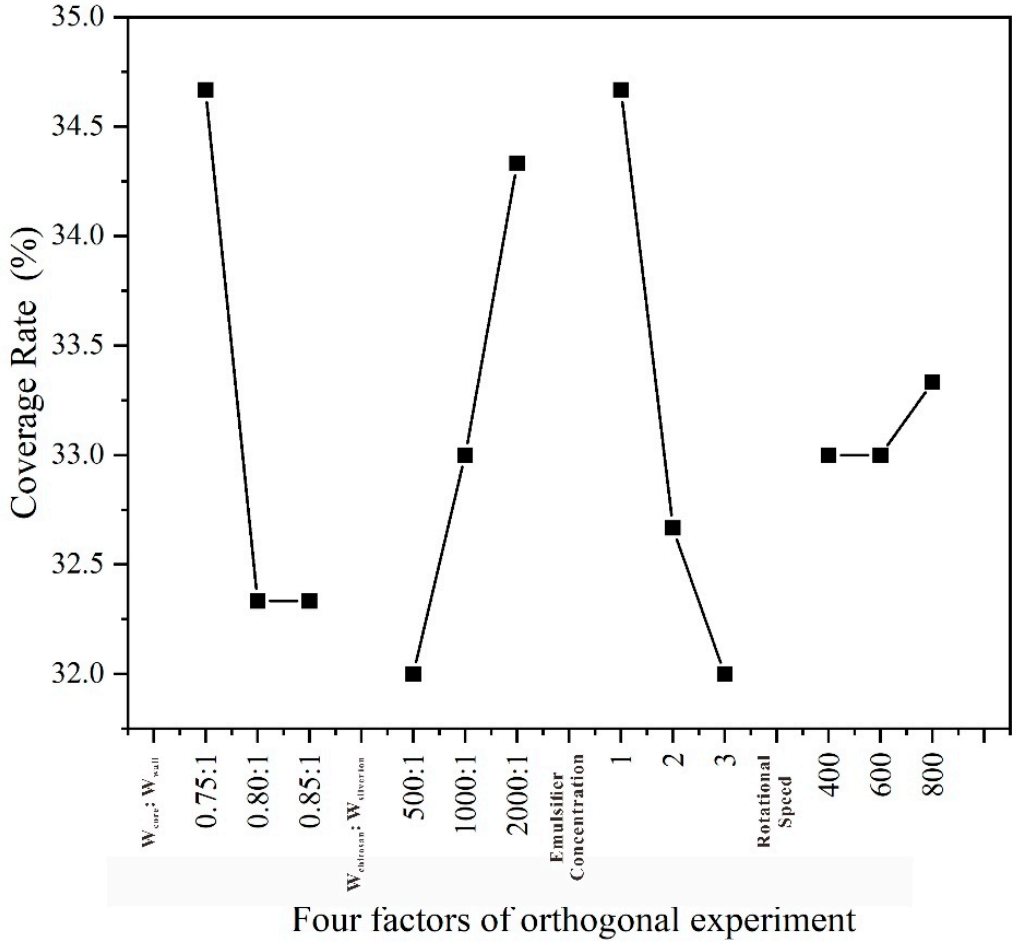

Figure 2. Effect curve of orthogonal experiment factors on coverage rate. The first line is effect of W_{core}/W_{wall} on coverage rate, the second line is effect of $W_{chitosan}/W_{silver\ ion}$ on coverage rate, the third line is effect of emulsifier concentration on coverage rate, the fourth line is curve of effect of rotational speed on coverage rate.

3.2. Analysis of Single-Factor Test Results of Microcapsules

3.2.1. Analysis of Output and Coverage Rate

As shown in Figure 3, eight groups of microcapsules with Span-80 concentrations of 0.5%, 1.0%, 1.5%, 2.0%, 2.5%, 3.0%, 4.0%, and 5.0%, respectively, were synthesized using the concentration of emulsifier as the variable. With the increasing concentration of emulsifier, the output of microcapsule trends was fluctuating, and the overall trend pattern was increasing. The graph of the coverage rate showed that the overall trend was incremental. The output of microcapsules prepared with emulsifier formulated in 0.5% increments was positively correlated with the coverage rate. The highest output was 14.94 g when the concentration of the emulsifier was 4.0%, followed by 14.71 g when the concentration of the emulsifier was 3.0%. When the concentrations of the emulsifier were 2.5% and 5.0%, the output amounts were 13.18 g and 12.4 g, respectively. The highest coverage rate was 44.0% when the emulsifier concentration was 4.0%, followed by 42.0% when the emulsifier concentration was 3.0%. The lowest coverage rate was 32.0% when the corresponding emulsifier concentration was 0.5%. When the microcapsules were prepared with 3.0% and 4.0% emulsifier, respectively, the high output and high coverage rate were obtained with low raw materials. Taking the sample prepared by a 4.0% emulsifier concentration (16 #) as an example, using the desiccator method, the formaldehyde emission was measured to be 0.291 mg/L, which was less than 1.5 mg/L as required by GB 18580-2001 [41], with a good air index.

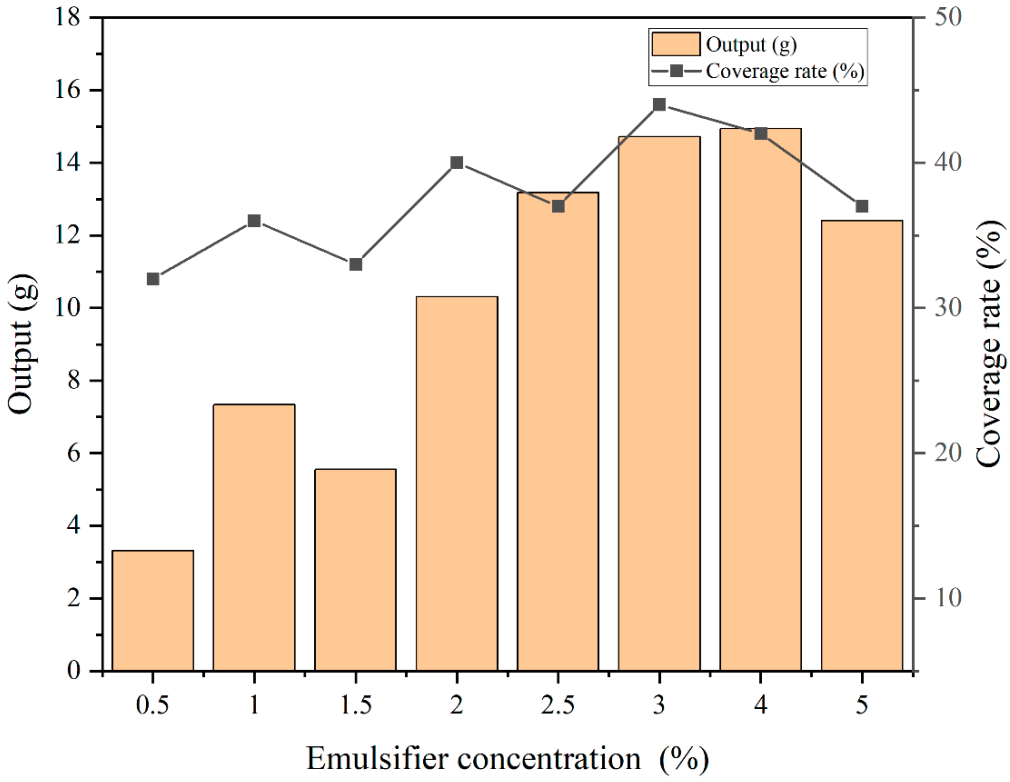

Figure 3. Relationship between the output and coverage rate of 8 groups of microcapsules in a single-factor experiment.

3.2.2. Analysis of Microscopic Morphology

The OM plots of the microscopic morphology of single-factor 8 groups of microcapsules are shown in Figure 4. The microcapsules of samples 10 # and 11 # prepared with a lower concentration of emulsifier had a uniform dispersion, but less quantity. Figure 4D shows that the dispersion of 13 # microcapsules prepared with a 2.0% concentration of emulsifier was better. The microcapsules of samples 14 # and 15 # were well dispersed. The microcapsules of samples 12 # and 17 # showed a large area of shading, and the agglomeration phenomenon was serious. In the extraction process, the dissolved chitosan solution was not covered by the MF wall and was not rinsed clean with deionized water and anhydrous ethanol, which is in the form of a gel. After drying, the microcapsules were basically in a lumpy state and required grinding. At this time, a large number of black microcapsules was observed under the microscope. It was not possible to observe the white dots at the core under an optical microscope according to the diffraction phenomenon of light. Therefore, the higher the concentration of the emulsifier, the better the morphology of the microcapsules. When the concentration of the emulsifier was 4.0%, the core material was fully emulsified. The water phase of chitosan-modified nano-silver solution was at the oil–water interface, and the core material was uniformly covered by the wall material.

Figure 5A shows the morphology of microcapsules of 11 # under a 2000× microscope, and Figure 5B shows the morphology of microcapsules under a 3000× microscope. With a low emulsifier concentration, the microcapsules were agglomerated with each other, and a small amount of core material was overflowed and uncoated. Figure 5C,D show the morphology of 14 # microcapsules under high and low magnification. Although the emulsifier concentration increased, and the microcapsule agglomeration was more obvious, the spherical shape of microcapsules was not round. The microcapsules prepared by low-concentration emulsifiers were more agglomerated and adhered to each other. Figure 5E,F show the morphology of 16 # microcapsules. The microcapsules prepared with an emulsifier concentration of 4.0% showed good dispersibility and good spherical

morphology, and microspheres were clearly seen under high magnification. Figure 5G,H show the microscopic morphology of 17 # microcapsules, with dense spheres. However, holes on the surface of the microcapsules were observed under the 3000× microscope (as shown by the red circles in Figure 5H). The reason for the depression was roughly that the density of the prepolymer of the MF was greater than the formaldehyde solution monomer, and different degrees of depression were formed at the oil–water interface during the coverage process. At the same time, the main reason for the existence of voids on the surface of the microcapsule may have been because of a rupture of the microcapsule due to capillary force during the high-temperature drying process. The SEM images show that the higher the emulsifier concentration, the better the microcapsule coverage effect.

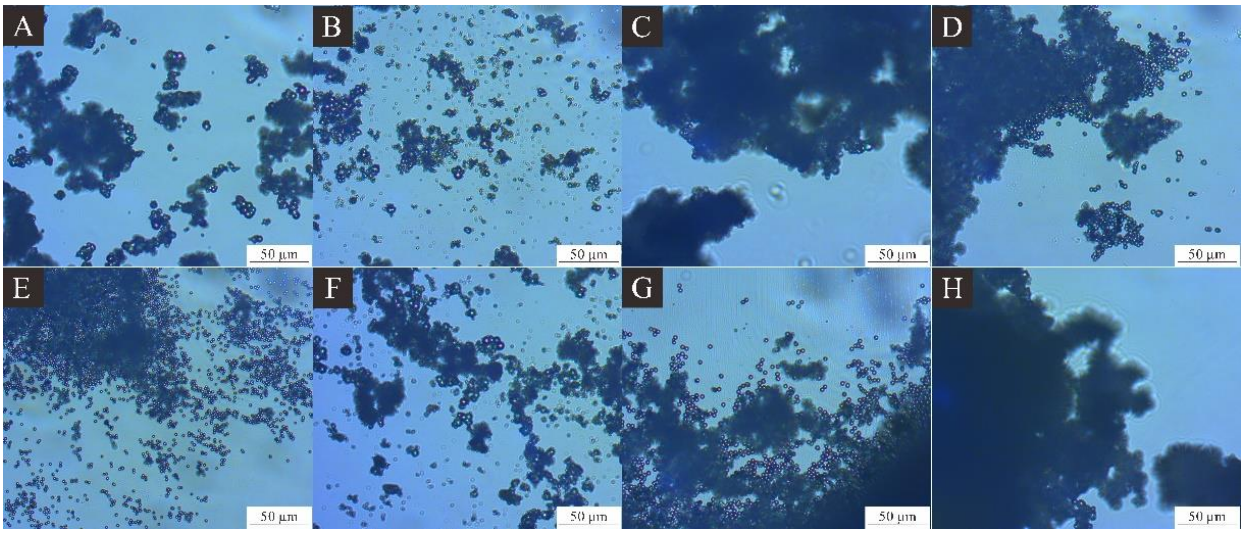

Figure 4. Optical microscope of 8 groups of microcapsules with different concentrations of emulsifier: (**A**) 0.5% for 10 #, (**B**) 1.0% for 11 #, (**C**) 1.5% for 12 #, (**D**) 2.0% for 13 #, (**E**) 2.5% for 14 #, (**F**) 3.0% for 15 #, (**G**) 4.0% for 16 #, (**H**) 5.0% for 17 #.

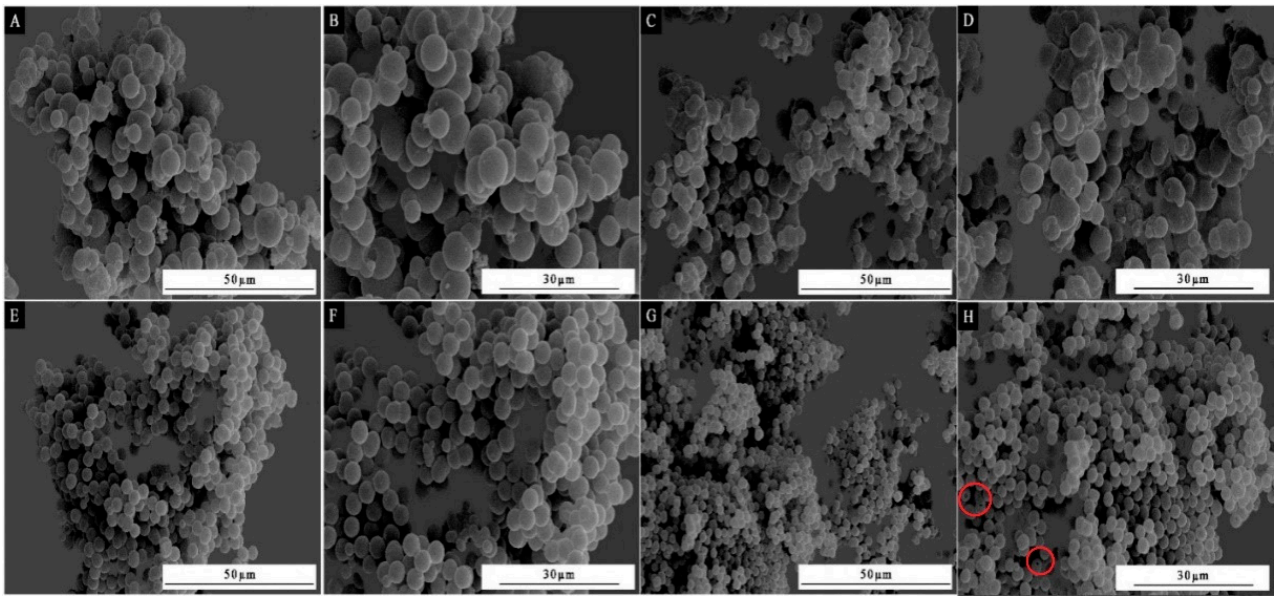

Figure 5. SEM images of microcapsules prepared with different emulsifier concentrations: (**A**) 11 # at 2000×, (**B**) 11 # at 3000×, (**C**) 14 # at 2000×, (**D**) 14 # at 3000×, (**E**) 16# at 2000×, (**F**) 16 # at 3000×, (**G**) 17 # at 2000×, (**H**) 17 # at 3000×, the red circles show holes on the surface of the microcapsules.

Figure 6 shows the particle size distribution of microcapsules prepared with different concentrations of emulsifier. Figure 6A shows that the particle size distribution range of microcapsules 11 # with an emulsifier concentration of 1.0% is mainly concentrated in 5–6 μm. Figure 6B shows that the particle size distribution range of microcapsules 14 # with an emulsifier concentration of 2.5% is mainly concentrated in 4–5 μm. Figure 6C shows that the particle size distribution range of microcapsules 16 # with an emulsifier concentration of 4.0% is mainly concentrated in 2.5–3 μm. Figure 6D shows that the particle size distribution range of microcapsules 17 # with an emulsifier concentration of 5.0% is mainly concentrated in 1.25–1.5 μm. With the increase in emulsifier concentration, the particle sizes of microcapsules showed a downward trend.

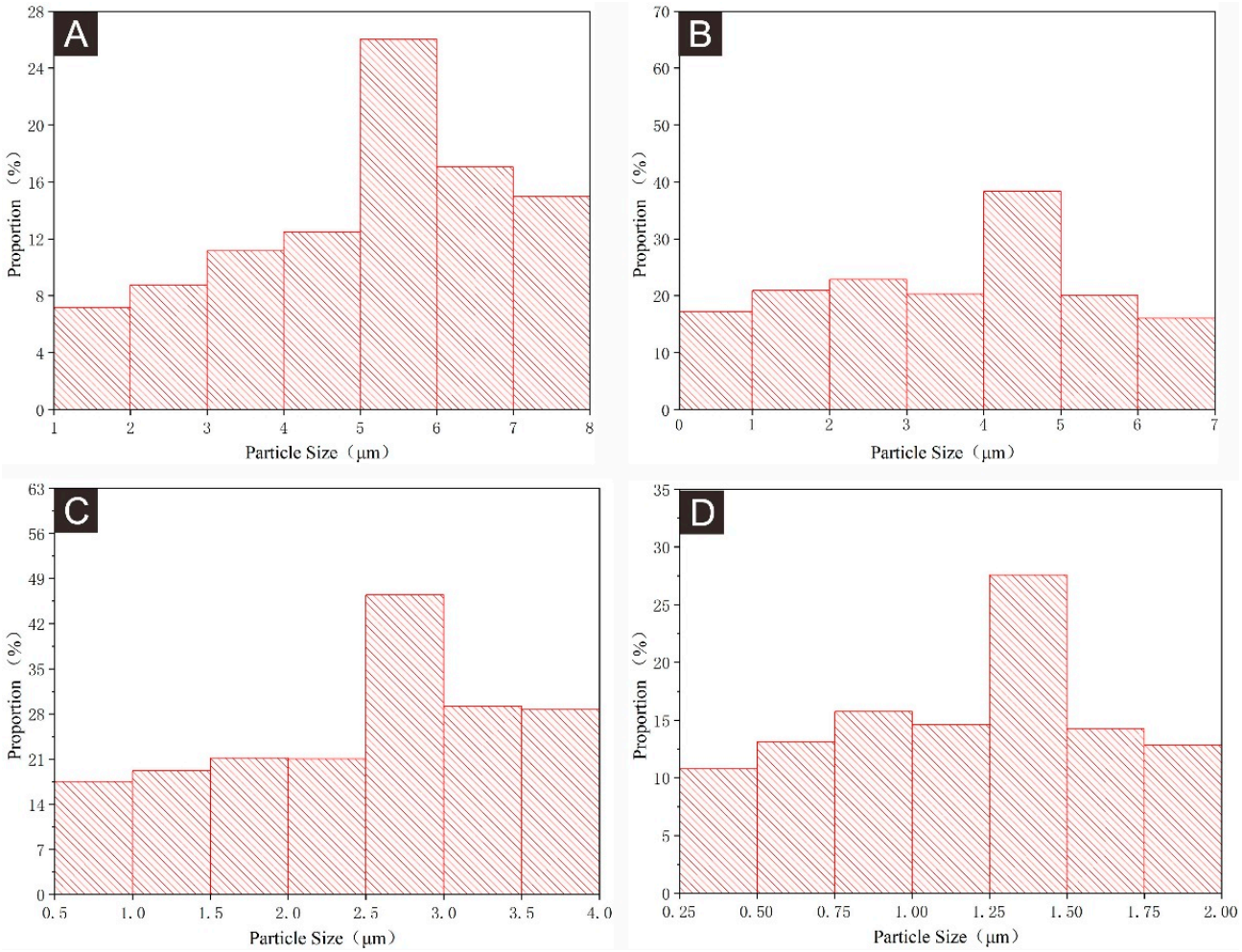

Figure 6. Particle size distribution of microcapsules prepared with different emulsifier concentrations: (**A**) 11 #, (**B**) 14 #, (**C**) 16 #, (**D**) 17 #.

3.2.3. Analysis of Chemical Composition of Microcapsules

As shown in Figure 7 of the infrared spectrum, the presence of the triazine ring vibration absorption peak at 813 cm^{-1} is the wall material of MF resin, and the absorption peak of C–O is 1000 cm^{-1}. The absorption peak of silver ions in nano-silver solution is 1330 cm^{-1}. The characteristic peak of chitosan O–H is 3432 cm^{-1}, and the O=C–O peak is 1640 cm^{-1}. There are overlapping N–H and O–H vibration peaks at 3425 cm^{-1} [42], indicating that O, N, and Ag^{+} in chitosan interact. Amino groups and hydroxyl groups in chitosan molecules can chemically modify silver ions, and the chitosan combined well with silver ions in nano-silver solution. It was proven that chitosan-modified nano-silver solution microcapsules were successfully prepared.

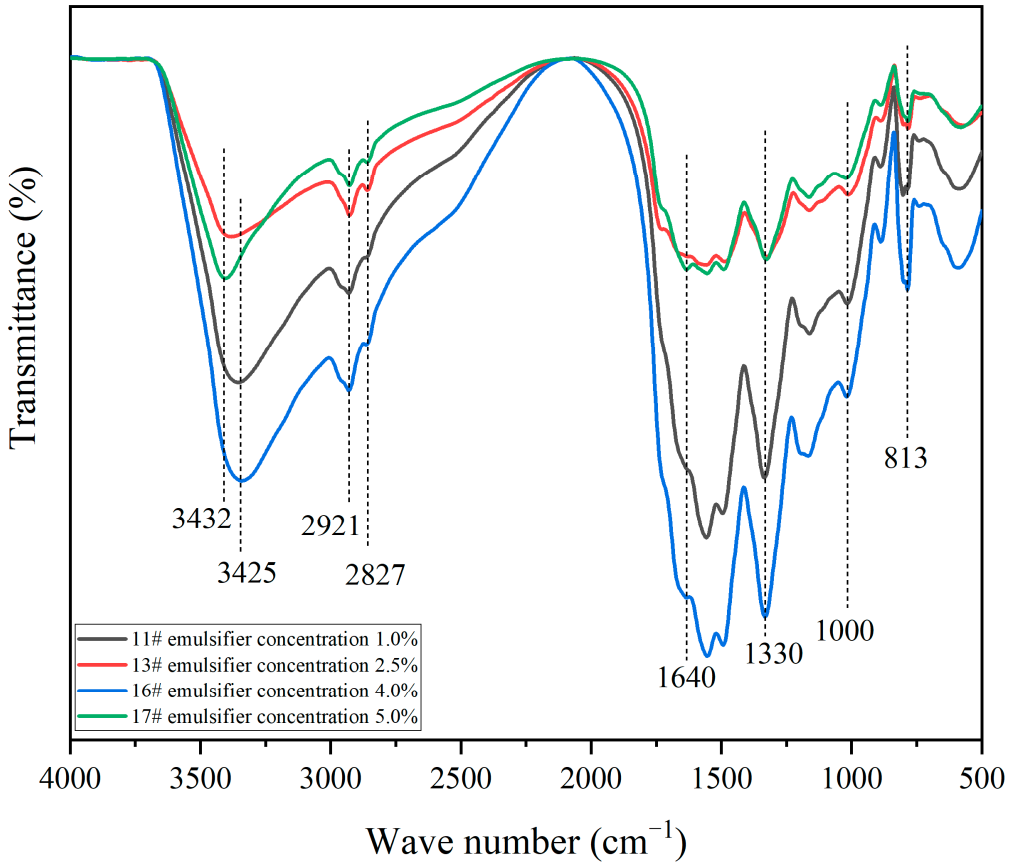

Figure 7. Infrared spectrum of microcapsules for single-factor test: 11 # emulsifier concentration of 1.0%, 13 # emulsifier concentration of 2.5%, 16 # emulsifier concentration of 4.0%, and 17 # emulsifier concentration of 5.0%.

3.3. Analysis of Optical Properties of Antibacterial Coating

3.3.1. Effect of Microcapsules with Different Emulsifier Concentrations on Gloss

Table 8 displays the gloss values of the coating on the surfaces of both substrates. The gloss of the coating has an important reference as an optical property of the coating. Gloss is the capacity to reflect light, and the gloss of the coating improves with the amount of light reflected. The gloss of the coating without adding microcapsules on the surface of glass substrate was 67.17%, and the gloss of the coating without adding microcapsules on the surface of Andoung wood was 45.37%. Figure 8 indicates the gloss (at 60°) trend of coating with microcapsules. When the concentration of emulsifier was 2.0%, the gloss of the coating was 14.77%. With the increasing concentration of emulsifier from 0.5% to 2.0%, the gloss of the coating on the glass substrate rose. As the concentration of emulsifier continued to rise, the gloss of the coating began to decline, from 10.5% to 5.1%. Similarly, the gloss of the coating on the surface of the Andoung wood increased with the increase in emulsifier concentration. The trend of gloss is thus firstly rising and then falling. When the emulsifier concentration was 2.0%, the gloss of the coating was 21.23%. When the emulsifier concentration reached 2.5%, the gloss of the coating declined. The microcapsules embedded in the coating increased the roughness of the surface of the coating, and the ability of the coating to reflect light at an incidence angle of 60° decreased, resulting in a decrease in the gloss of the coating.

Table 8. The gloss of coatings on different substrates.

Sample (#)	Emulsifier Concentration (%)	Gloss of Glass Substrate (%)			Gloss of Andoung Wood (%)		
		20°	60°	85°	20°	60°	85°
10	0.5	2.03	6.73	4.00	4.00	16.63	15.20
11	1.0	2.23	7.00	1.87	1.50	18.17	5.40
12	1.5	2.77	9.83	6.40	4.80	21.20	27.53
13	2.0	1.77	14.77	1.90	5.03	21.23	23.70
14	2.5	2.93	10.50	6.97	3.73	16.90	18.43
15	3.0	2.30	7.70	3.10	2.37	11.03	9.70
16	4.0	2.00	6.43	2.30	4.07	8.27	10.90
17	5.0	6.10	5.10	2.10	5.23	21.03	29.87

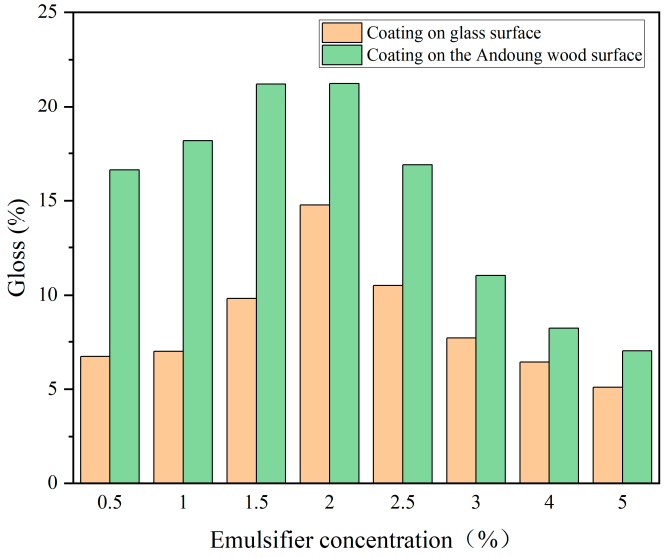

Figure 8. Gloss of coating on glass and wood substrates: 10 # emulsifier concentration 0.5%, 11 # emulsifier concentration 1.0%, 12 # emulsifier concentration 1.5%, 13 # emulsifier concentration 2.0%, 14 # emulsifier concentration 2.5%, 15 # emulsifier concentration 3.0%, 16 # emulsifier concentration 4.0%, 17 # emulsifier concentration 5.0%.

When the emulsifier concentration was greater than 2.0%, the gloss of coating on both substrates was reduced, probably because the microcapsules added to the waterborne coating as filler affected the gloss of the coating. The chitosan-modified nano-silver solution microcapsules are in the form of white powder. When mixed with waterborne coating with a 4.0% microcapsule content, the ability of the coating to reflect light was reduced. Therefore, the gloss of the coating on the substrate was reduced. The gloss of the coating on wood surface was superior to that on the glass substrate, which means that the coating itself has gloss and the antibacterial coating does not affect the gloss of the coatings on wood surface.

3.3.2. Effect of Microcapsules with Different Emulsifier Concentrations on Color Difference

Chromaticity is a reference value used to measure the color difference and uniformity of the coating [43]. Table 9 shows the chromaticity values of the coating on the surface of glass substrates and the Andoung wood. On the surface of the glass substrate, the "*L*" value of the coating without the addition of microcapsules was 68.47, the "*a*" value was 2.1, the "*b*" value was 8, the "*c*" value was 8.23, and the "*H*" value was 74.83. As shown in Figure 9, the color difference values of the coating were obtained according to the color difference calculation method. With the increase in emulsifier concentration, compared with the coating without the addition of microcapsules, the color difference values of 10 # to 17 # coatings show a fluctuating trend. The reason was that the microcapsules adhered to

bristles when the prepared antibacterial coating was dipped into with a brush. This led to the accumulation of microcapsules in one place during the process of painting, increasing the roughness of the coating. There is no clear trend in the color difference of coating on the surface of glass. The samples of 12 #, 16 #, and 17 # had smaller color differences compared with the surface of the coating without adding microcapsules, and the color difference values were 2.61, 2.91, and 2.18, respectively. On the surface of the Andoung wood, 12 #, 16 #, and 17 # had smaller color differences compared with the surface of the coating without microcapsules, and the color difference values were 13.26, 13.66, and 14.29, respectively. The color difference of the coating on the surface of the Andoung wood was much higher than the that on the surface of glass substrate, because the Andoung wood itself had a red-brown wood grain texture. The *a* value indicates the red-green difference, and the *a* value of the coating on the surface of wood will be significantly higher than that of the coating on the surface of glass substrate, so the overall color difference values of the coating on Andoung wood were higher.

Table 9. Color difference values of coating on different substrates.

Substrate	Sample (#)	*L*	*a*	*b*	*c*	*H*	Δ*E*
Glass	10	68.40	1.40	6.63	6.80	77.87	4.95
	11	63.70	0.67	6.23	6.30	83.70	5.28
	12	66.53	0.70	6.93	6.97	83.40	2.61
	13	68.60	1.10	6.70	6.50	83.70	6.97
	14	65.23	0.43	7.43	7.43	86.33	3.68
	15	65.83	0.70	7.20	7.20	84.03	7.89
	16	66.27	0.77	6.63	6.67	83.13	2.91
	17	66.77	0.87	7.40	7.47	82.93	2.18
Andoung Wood	10	49.93	12.10	19.90	23.4	58.53	24.10
	11	47.87	18.9	21.37	28.53	48.50	20.30
	12	40.83	24.17	34.23	42.00	54.60	13.26
	13	43.30	19.10	29.90	32.00	54.83	18.97
	14	46.10	15.27	29.13	32.93	62.23	21.72
	15	45.80	18.33	26.10	32.00	54.83	20.88
	16	36.50	21.60	30.57	37.53	54.53	13.66
	17	41.90	23.17	33.97	41.13	55.57	14.29

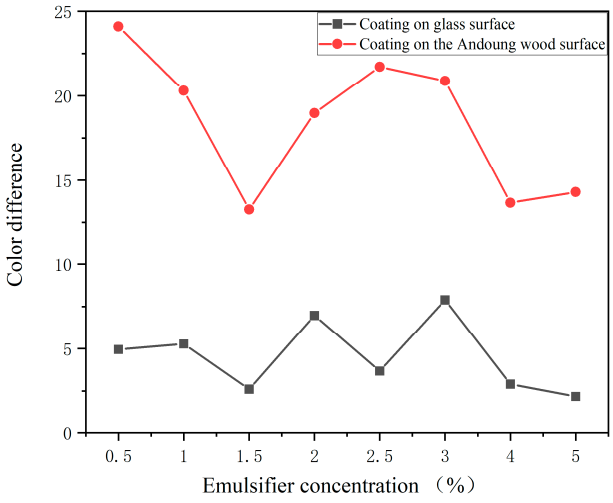

Figure 9. Change trend of color difference on the surface of glass and wood: 10 # emulsifier concentration 0.5%, 11 # emulsifier concentration 1.0%, 12 # emulsifier concentration 1.5%, 13 # emulsifier concentration 2.0%, 14 # emulsifier concentration 2.5%, 15 # emulsifier concentration 3.0%, 16 # emulsifier concentration 4.0%, 17 # emulsifier concentration 5.0%.

3.3.3. Effect of Microcapsules with Different Emulsifier Concentrations on Light Transmission

Figure 10 shows the UV–Vis transmission spectra of the coatings. Since the waterborne primer is colorless and transparent, mixing the microcapsules with waterborne primer may reduce the transparency of the coating. The transmittance of the coating in the visible light range of 300−800 nm was tested with a UV spectrometer. The transmittance of coating without adding microcapsules was up to 96.1%, and the transmittance of coatings decreased with the addition of microcapsules. The 10 # coating had only a 93.1% transmittance, which indicated that the microcapsules affected the transparency of the coating, and the change of emulsifier concentration affected the particle size of microcapsules and the roughness of the coating surface. When the emulsifier concentration was 2.0%, the coating transmittance of 13 # decreased to 88.5%, which was much lower than the transmittance of the coating. When the emulsifier concentrations were 4.0% and 5.0%, respectively, the transmittance of the coating was the same, at 84.0%. The overall trend of the transmittance of the eight groups of coatings was negatively correlated with the concentration of the emulsifier. This is due to the phenomenon of phase separation caused by the addition of microcapsules as polymers into waterborne coatings, which increased the roughness of the coating surface and the refraction of light [44]. Therefore, the addition of microcapsules to waterborne primers should ensure that the emulsifier concentration does not exceed 2.0%, so as to show excellent transparency.

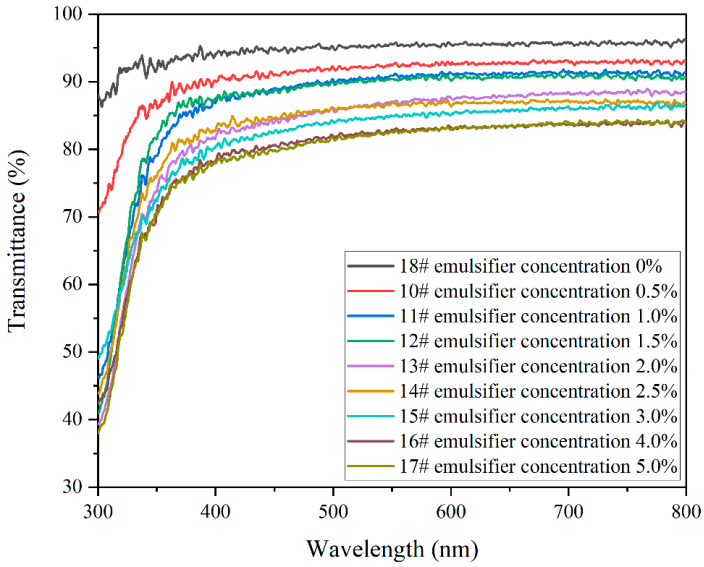

Figure 10. Trend of coating transparency measured by ultraviolet spectrometer.

3.4. Analysis of the Mechanical Properties of Antibacterial Coating

The hardness, adhesion, and impact resistance of antibacterial coatings prepared with different concentrations of emulsifiers are shown in Table 10. The mechanical properties of the coating determine the overall stability of the material, where the hardness is associated with the internal composition structure of the material. The hardness of the coating without the addition of microcapsules was 2H, and as the concentration of the emulsifier increased, the hardness of the coating first became as strong as 4H, then reached 3H and finally stabilized. When the concentration of the emulsifier was 2.0%, the hardness was 3H. The main reason is that the addition of microcapsules led to agglomeration, which led to stress concentration on the surface of the coating. The subsequent decrease in the hardness of the coating is due to the fact that the microcapsules themselves may be thin-walled or hollow, resulting in a decrease in hardness. Therefore, the microcapsules as fillers affected the hardness of the coating.

Table 10. Mechanical properties of coating on the surface of the Andoung wood.

Sample (#)	Emulsifier Concentration (%)	Hardness (H)	Adhesion (Level)	Impact Strength (kg·cm)	Roughness (μm)
18	0	2	1	15	0.38
10	0.5	3	3	27	3.39
11	1.0	4	3	31	4.49
12	1.5	4	2	25	3.20
13	2.0	3	2	25	2.89
14	2.5	3	2	24	2.61
15	3.0	3	1	20	2.55
16	4.0	3	1	20	2.29
17	5.0	3	1	18	1.74

Adhesion is a mechanical property that characterizes the interface between coating and wood. The adhesion ability of the coating without adding microcapsules was good, up to level 1, but as the concentration of emulsifier increased, the adhesion of the coating decreased; for example, the adhesion of 11 # was level 3. The main reason for the decrease in the adhesion of the coating surface is the agglomeration after adding microcapsules to the waterborne coatings. Due to the different dispersibility of microcapsules in coatings, when applied on the surface of wood, the gaps between the coating and wood increases and the contact surface decreases. When the coating was subjected to force, it produced peeling, and the corresponding adhesion was reduced. When the emulsifier concentration was 3.0%−5.0%, the adhesion level of the coating was 1 at this time.

Another important parameter characterizing the mechanical properties was the impact resistance. The impact resistance of the coating without the addition of microcapsules was only 15 kg·cm, but with the addition of microcapsules, the mechanical properties of the coating significantly improved. As the concentration of the emulsifier increased, when the microcapsules were added to the waterborne coatings, the impact strength of the coating also increased. The impact resistance of 11 # was 31 kg·cm, which is the highest value. When the emulsifier concentrations were 3.0% and 4.0%, respectively, the impact resistance was 20 kg·cm. The addition of microcapsules to waterborne coating increases the impact strength of the coating [45]. When the small hammer falls, the wall of the microcapsules also disperses a part of the impact force, thus increasing the impact strength of the coating as a whole. Therefore, when the concentration of the emulsifier is higher, the microcapsule coating is more effective, and the impact resistance is improved. Once the microcapsules exhibited the agglomeration phenomenon and were added to the coating, when subjected to impact force, the microcapsules were unable to disperse a portion of the force, but rather weakened the impact resistance.

The roughness of the surface of the coating is shown in Table 10. The surface of the coating without adding microcapsules was smooth and flat, and the roughness of the coating increased with the addition of microcapsules. But as the emulsifier concentration rose, the coating roughness showed a decreasing trend. When the emulsifier concentration was 5.0%, the coating roughness at this time was 1.74 μm. This indicates that as the emulsifier concentration increased, the core material was emulsified into small droplets at the oil–water interface, which was covered by the wall material and affected the particle size of the microcapsules. Therefore, the microcapsules are not dispersed evenly in the antibacterial coating, and the coating with the addition of microcapsules on the surface of wood forms a large area of agglomeration, which affects the roughness of the coating.

3.5. Effect of Microcapsules with Different Emulsifier Concentrations on Antibacterial Properties

Figure 11 shows the trend of the antibacterial properties of the coating on a glass substrate against *Escherichia coli* and *Staphylococcus aureus*. For *Escherichia coli*, the antibacterial property of the coating increased as the concentration of the emulsifier increased. When the emulsifier content was 0.5%, the antibacterial rate was 64.4%, and when the

emulsifier concentration was 4.0%, the antibacterial rate of the coating reached a maximum of 80.0%. For *Staphylococcus aureus*, the trend of change was the same as the former. When the content of the emulsifier reached 4.0%, the antibacterial rate of the coating reached a maximum of 71.3%, and then decreased. The trend of antibacterial properties of coating on Andoung wood surface against *Escherichia coli* and *Staphylococcus aureus* is shown in Figure 12. When the emulsifier concentration reached 4.0%, the antibacterial rate reached a maximum of 73.2%, followed by a decline. It showed that the that excessive concentration of the emulsifier may reduce the antibacterial property of the coating. For *Staphylococcus aureus*, when the emulsifier concentration continued to grow, the antibacterial properties of the coating increased. When the emulsifier concentration reached 4.0%, the antibacterial rate reached the maximum value of 68.4% and then decreased. It can be concluded that a high concentration of the emulsifier can fully emulsify the core material. When the condensation reaction occurs, the wall material can cover the core material. When the emulsifier concentration was 4.0% to reach the critical value, the stability of the emulsion system was the best.

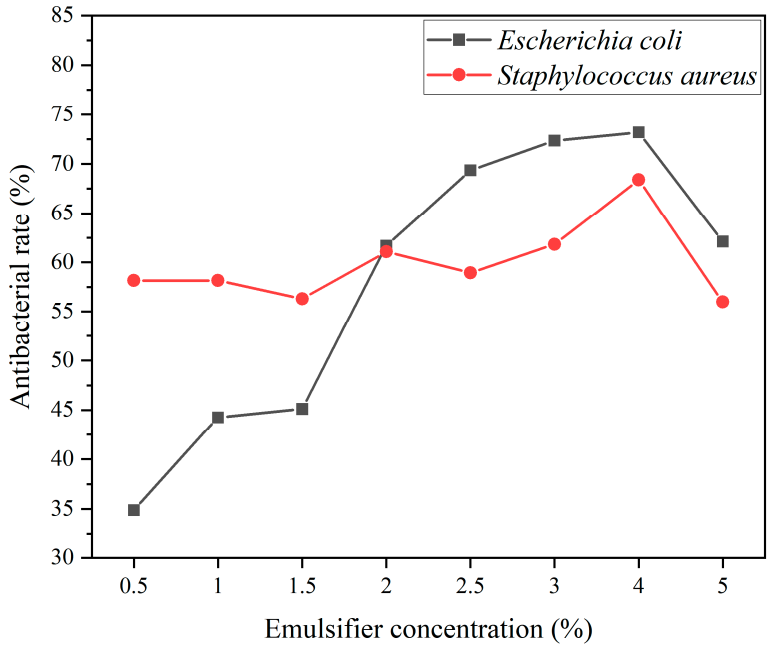

Figure 11. The antibacterial rate of coating on glass substrate.

The antibacterial properties of the coating on the surfaces of the two groups of substrates were compared. It was found that the antibacterial properties of coating on the glass substrate were better than those on the surface of the Andoung wood. Due to the presence of chitosan and nano-silver solutions in the coating, the chitosan and nano-silver solutions have an adsorption effect on bacteria [46], disrupting the structure of bacteria and achieving antibacterial effects. It is indicated that the coating itself has an antibacterial property, and the reason for the decrease in the antibacterial property of the coating on the wood surface is that it is easy to breed bacteria on wood [47]. The antibacterial mechanism of chitosan-modified nano-silver solution microcapsules is mainly related to the walls of the microcapsules, which comprise an incomplete sealing structure with micropores on the surface. The antibacterial agent of the core is released through the micropores and reacts with the bacteria to achieve the effect of bacterial inhibition.

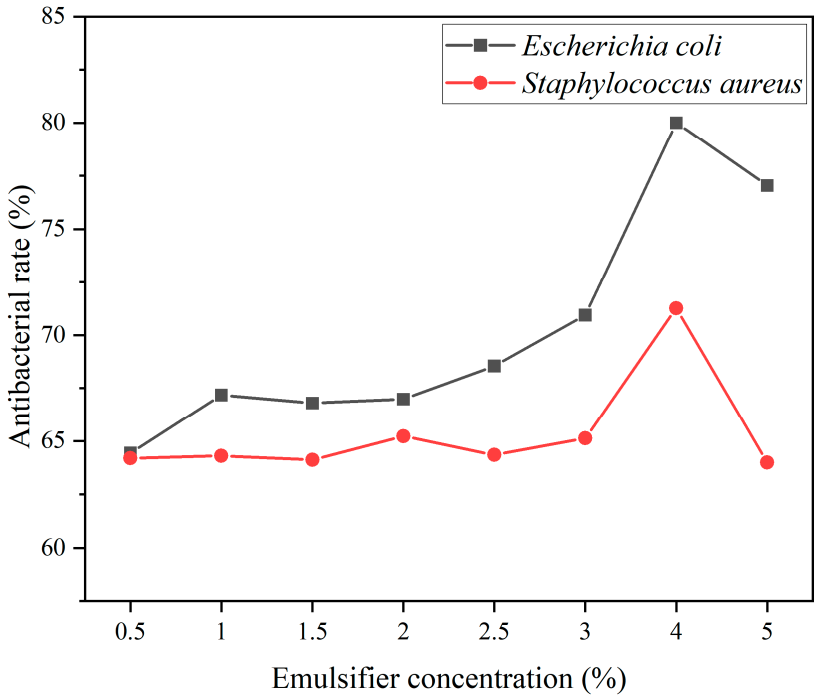

Figure 12. Antibacterial rate of coating on surface of the Andoung wood.

3.6. Comparison Analysis before and after Antibacterial Tests

The chemical composition of the coating before and after antibacterial tests was compared with the optimal antibacterial sample 16 # with an emulsifier concentration of 4.0% to investigate whether the antibacterial tests affected the microstructure of the coating. Figure 13 shows the infrared spectra of sample 16 # before and after antibacterial tests. The chemical composition of sample 16 # without antibacterial tests and after antibacterial tests against *Escherichia coli* and *Staphylococcus aureus* was tested. As a whole, the overall stretching peaks of the three coatings showed the same trend, with the triazine ring vibration absorption peak of MF resin at 813 cm^{-1}. The absorption peaks of silver ions in nano-silver solution are 1330 cm^{-1} and 2921 cm^{-1}. The main characteristic peak of chitosan was the stretching peak at 1619 cm^{-1} [48]. No new substances were generated in the chemical composition of the coating before and after antibacterial tests. The antibacterial coating did not react with bacteria.

Figure 14 compares the surface of coating on the Andoung wood before and after antibacterial tests. Figure 14A–C show the coating with 16 # antibacterial microcapsules. The surface of the coating before antibacterial tests was smooth and flat, and white particles of the microcapsules were seen. The antibacterial effect of the coating for *Escherichia coli* was good, and the bacteria breeding on the surface of the coating was less. The antibacterial effect for *Staphylococcus aureus* was weaker, and more bacteria were bred on the surface of the coating. The coating without microcapsules is shown in Figure 14D–F. The coating without chitosan-modified nano-silver solution microcapsules was prone to bacteria-breeding, and a small amount of bacteria had appeared before antibacterial tests. When *Escherichia coli* and *Staphylococcus aureus* were inoculated to the coating on the wood surface, the coating had a large area of bacteria. Therefore, the chitosan-modified nano-silver solution microcapsules have antibacterial properties, and their antibacterial effect on *Escherichia coli* is superior to that of *Staphylococcus aureus* because the cell wall structure of *Escherichia coli* consists of proteins, lipids, and lipopolysaccharides [49], which have a certain resistance to the external environment and are able to protect themselves. In contrast, *Staphylococcus aureus* does not contain an outer membrane envelope and loses its own protective effect [50]. Therefore, the chitosan-modified nano-silver solution microcapsules were added to coatings and applied

on the surface of the Andoung wood, exhibiting antibacterial properties against *Escherichia coli* and *Staphylococcus aureus*.

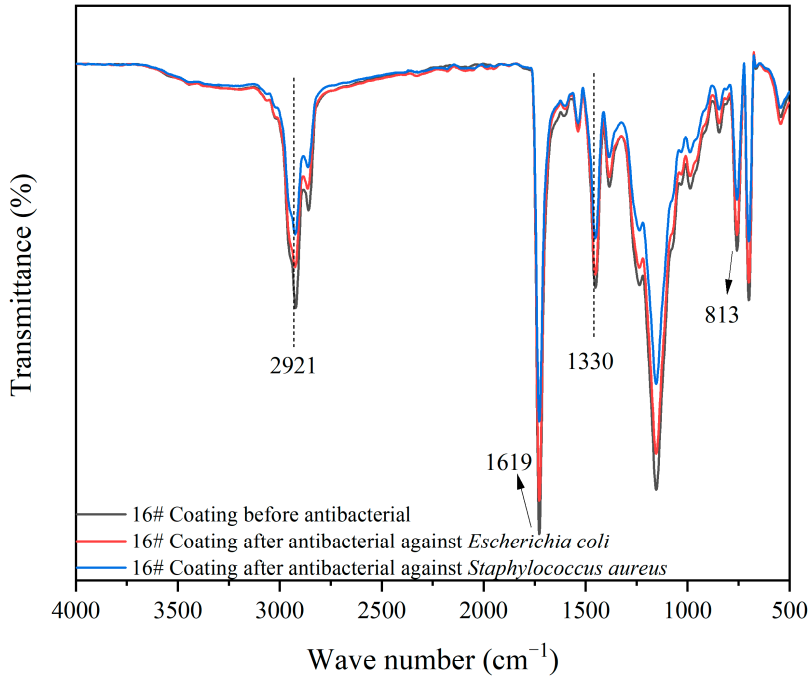

Figure 13. Infrared spectrum of coating (16 #) on the Andoung wood.

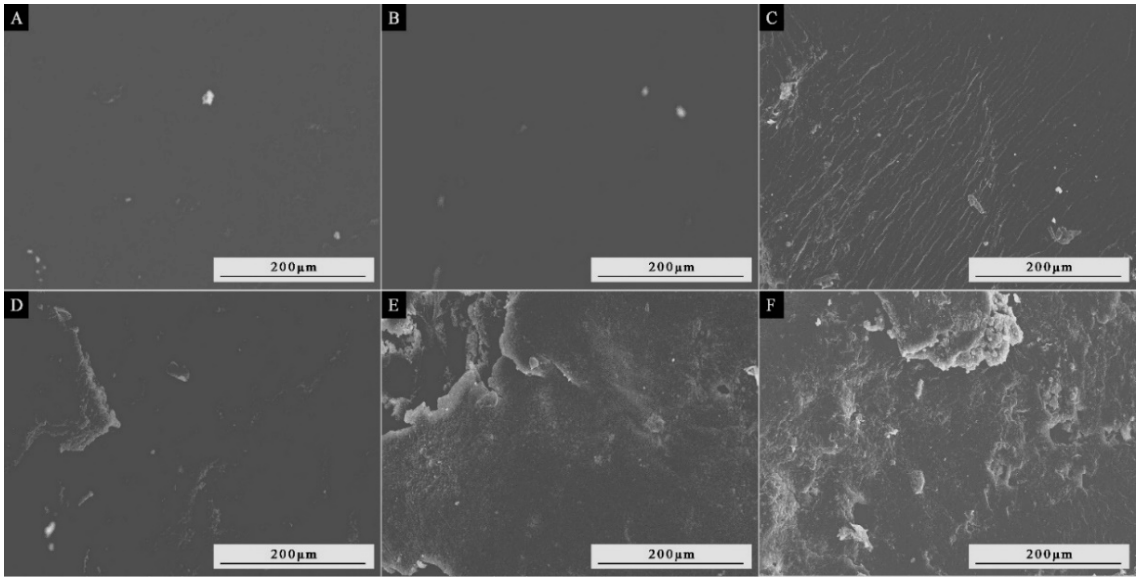

Figure 14. SEM of the coating on Andoung wood before and after antibacterial tests: 16 # coating (**A**) before antibacterial test, (**B**) after antibacterial test against *Escherichia coli*, and (**C**) after antibacterial test against *Staphylococcus aureus*; coating without adding microcapsules (**D**) before antibacterial test, (**E**) after antibacterial test against *Escherichia coli*, and (**F**) after antibacterial test against *Staphylococcus aureus*.

4. Conclusions

According to the results of the orthogonal experiment, the emulsifier concentration was positively connected with the overall output and coverage rate of chitosan-modified nano-silver solution microcapsules. The antibacterial coating was prepared by mixing microcapsules with waterborne primer at a content of 4.0%. Then, the coating was coated

on glass and wood substrates, respectively, and the optical, mechanical, and antibacterial properties of the coating were tested. The gloss of the coating first increased and then decreased with the concentration of the emulsifier. When the emulsifier concentration was 2.0%, the maximum values reached 21.23% on the surface of the Andoung wood. The change of the emulsifier concentration had little effect on the color difference of coating. When the emulsifier concentrations were 1.5%, 4.0%, and 5.0%, respectively, the color differences of coating on wood surface were smaller, at 13.26, 13.66, and 14.39, respectively. The light transmittance of the coating was negatively correlated with the concentration of the emulsifier. The hardness of the coating first increased with the concentration of the emulsifier and then decreased. When the concentration of the emulsifier exceeded 2.0%, the hardness of the coating decreased to 3H and remained unchanged. The highest impact resistance of the coating was 31 kg·cm when the emulsifier concentration was 1.0%. When the concentration of the emulsifier was 3.0%–5.0%, the adhesion of the coating reached level 1. When the concentration of the emulsifier was 5.0%, the roughness of the coating was 1.74 μm. When the concentration of the emulsifier reached 4.0%, the antibacterial rates against *Escherichia coli* and *Staphylococcus aureus* reached their highest values, which were 71.3% and 80.0%, respectively, on the surface of the glass substrate, and 68.4% and 73.2%, respectively, on the surface of the Andoung wood. By analyzing the chemical composition of the coating, no new materials were produced before and after antibacterial tests. The chitosan-modified nano-silver solution microcapsules can be embedded into coatings and applied to wood surfaces, broadening their potential use in coatings and other fields.

Author Contributions: Conceptualization, methodology, validation, resources, data management, and supervision, Y.W., writing—review and editing, P.P., and formal analysis, investigation, X.Y. All authors have read and agreed to the published version of the manuscript.

Funding: This project was partly supported by the Postgraduate Research and Practice Innovation Program of Jiangsu Province (SJCX23_0324) and the Natural Science Foundation of Jiangsu Province (BK20201386).

Institutional Review Board Statement: Not applicable.

Informed Consent Statement: Not applicable.

Data Availability Statement: Not applicable.

Conflicts of Interest: The authors declare no conflict of interest.

References

1. Hu, W.G.; Liu, N.; Xu, L.; Guan, H.Y. Study on cold/warm sensation of materials used in desktop of furniture. *Wood Res. Slovak.* **2020**, *65*, 497–506. [CrossRef]
2. Luo, Z.Y.; Xu, W.; Wu, S.S. Performances of Green Velvet Material (PLON) Used in Upholstered Furniture. *Bioresources* **2023**, *18*, 5108–5119. [CrossRef]
3. Luo, Y.R.; Xu, W. Optimization of Panel Furniture Plates Rework Based on Intelligent Manufacturing. *Bioresources* **2023**, *18*, 5198–5208. [CrossRef]
4. Hu, W.G.; Luo, M.Y.; Hao, M.M.; Tang, B.; Wan, C. Study on the effects of selected factors on the diagonal tensile strength of oblique corner furniture joints constructed by wood dowel. *Forests* **2023**, *14*, 1149. [CrossRef]
5. Singh, A.P.; Kim, Y.S.; Chavan, R.R. Relationship of wood cell wall ultrastructure to bacterial degradation of wood. *Iawa J.* **2019**, *40*, 845–870. [CrossRef]
6. Xu, W.; Chen, P.; Yang, Y.; Wang, X.; Liu, X. Effects of freezing and steam treatments on the permeability of Populus tomentosa. *Mater. Werkst.* **2021**, *52*, 907–915. [CrossRef]
7. Yang, Y.Q.; Xu, W.; Liu, X.; Wang, X.D. Study on permeability of cunninghamia lanceolata based on steam treatment and freeze treatment. *Wood Res.* **2021**, *66*, 721–731. [CrossRef]
8. Li, R.R.; Fang, L.; Xu, W.; Xiong, X.; Wang, X.D. Effect of laser irradiation on the surface wettability of poplar wood. *Sci. Adv. Mater.* **2019**, *11*, 655–660. [CrossRef]
9. Wang, J.J.; Lu, Y.Z.; Chu, Q.D.; Ma, C.L.; Cai, L.R.; Shen, Z.H.; Chen, H. Facile construction of superhydrophobic surfaces by coating fluoroalkylsilane/silica composite on a modified hierarchical structure of wood. *Polymers* **2022**, *12*, 813. [CrossRef]
10. Rosu, L.; Varganici, C.D.; Mustata, F.; Rosu, D.; Rosca, I.; Rusu, T. Epoxy coatings based on modified vegetable oils for wood surface protection against fungal degradation. *ACS Appl. Mater. Inter.* **2020**, *12*, 14443–14458. [CrossRef]

11. Hu, W.G.; Yu, R.Z. Mechanical and acoustic characteristics of four wood species subjected to bending load. *Maderas-Cienc. Tecnol.* **2023**, *25*, 39.
12. Hu, W.G.; Yu, R.Z.; Luo, M.Y.; Konukcu, A.C. Study on tensile strength of single dovetail joint: Experimental, numerical, and analytical analysis. *Wood Mater. Sci. Eng.* **2022**, *17*, 2155875. [CrossRef]
13. Zhang, S.W.; Yu, A.X.; Song, X.Q.; Liu, X.Y. Synthesis and characterization of waterborne UV-curable polyurethane nanocomposites based on the macromonomer surface modification of colloidal silica. *Prog. Org. Coat.* **2013**, *76*, 1032–1039. [CrossRef]
14. Zafar, F.; Ghosal, A.; Sharmin, E.; Chaturvedi, R.; Nishat, N. A review on cleaner production of polymeric and nanocomposite coatings based on waterborne polyurethane dispersions from seed oils. *Prog. Org. Coat.* **2019**, *131*, 259–275. [CrossRef]
15. Jiang, G.F.; Li, X.F.; Che, Y.L.; Lv, Y.; Liu, F.; Wang, Y.Q.; Zhao, C.C.; Wang, X.J. Antibacterial and anticorrosive properties of CuZnO@RGO waterborne polyurethane coating in circulating cooling water. *Environ. Sci. Pollut. Res.* **2019**, *26*, 9027–9040. [CrossRef]
16. Zare, E.N.; Padil, V.V.T.; Mokhtari, B.; Venkateshaiah, A.; Waclawek, S.; Cernik, M.; Tay, F.R.; Varma, R.S.; Makvandi, P. Advances in biogenically synthesized shaped metal- and carbon-based nanoarchitectures and their medicinal applications. *Adv. Colloid Interfac.* **2020**, *283*, 102236. [CrossRef]
17. Matineh, G.; Ali, Z.; Reza, M.; Zahra, B.T.; Milad, A.; Ehsan, N.Z.; Tarun, A.; Vinod, V.T.P.; Babak, M.; Filippo, R.; et al. Functionalization of Polymers and Nanomaterials for Biomedical Applications: Antimicrobial Platforms and Drug Carriers. *Prosthesis* **2020**, *2*, 117–139.
18. Harvey, A.L. Natural products in drug discovery. *Drug Discov. Today* **2008**, *13*, 894–901. [CrossRef]
19. Li, L.; Lu, Y.A.; Chen, Y.; Bian, J.Y.; Wang, L.; Li, L. Antibacterial Chitosan-Gelatin Microcapsules Modified with Green-Synthesized Silver Nanoparticles for Food Packaging. *J. Renew. Mater.* **2023**, *11*, 291–307. [CrossRef]
20. Wahab, M.A.; Li, L.M.; Matin, M.A.; Karim, M.R.; Aijaz, M.O.; Alharbi, H.F.; Abdala, A.; Haque, R. Silver Micro-Nanoparticle-Based Nanoarchitectures: Synthesis Routes, Biomedical Applications, and Mechanisms of Action. *Polymers* **2021**, *13*, 2870. [CrossRef]
21. Tang, S.H.; Zheng, J. Antibacterial Activity of Silver Nanoparticles: Structural Effects. *Adv. Healthc. Mater.* **2018**, *7*, 1701503. [CrossRef] [PubMed]
22. Ciriminna, R.; Albo, Y.; Pagliaro, M. New Antivirals and Antibacterials Based on Silver Nanoparticles. *ChemMedChem* **2020**, *15*, 1619–1623. [CrossRef] [PubMed]
23. Hamad, A.; Khashan, K.S.; Hadi, A. Silver Nanoparticles and Silver Ions as Potential Antibacterial Agents. *J. Inorg. Organomet. Polym. Mater.* **2020**, *30*, 4811–4828. [CrossRef]
24. Joy, F.; Devasia, J.; Nizam, A.; Lakshmaiah, V.V.; Krishna, S.B.N. Fungi-Templated Silver Nanoparticle Composite: Synthesis, Characterization, and Its Applications. *Appl. Sci.* **2023**, *13*, 2158. [CrossRef]
25. Pan, P.; Yan, X.X. Preparation of Antibacterial Nanosilver Solution Microcapsules and Their Impact on the Performance of Andoung Wood Surface Coating. *Polymers* **2023**, *15*, 1722. [CrossRef]
26. Anuj, S.A.; Gajera, H.P.; Hirpara, D.G.; Golakiya, B.A. Bacterial membrane destabilization with cationic particles of nano-silver to combat efflux-mediated antibiotic resistance in Gram-negative bacteria. *Life Sci.* **2019**, *230*, 178–187. [CrossRef] [PubMed]
27. Vatcharakajon, P.; Sornsaket, A.; Choengpanya, K.; Susawaengsup, C.; Sornsakdanuphap, J.; Boonplod, N.; Bhuyar, P.; Dangtungee, R. Silver Nano Chito Oligomer Hybrid Solution for the Treatment of Citrus Greening Disease (CGD) and Biostimulants in Citrus Horticulture. *Horticulturae* **2023**, *9*, 725. [CrossRef]
28. El-Shamy, O.A.A.; Deyab, M.A. Novel anticorrosive coatings based on nanocomposites of epoxy, chitosan, and silver. *Mate. Lett.* **2023**, *330*, 133298. [CrossRef]
29. Nian, L.Y.; Xie, Y.; Sun, X.Y.; Wang, M.J.; Cao, C.J. Chitosan quaternary ammonium salt/gelatin-based biopolymer film with multifunctional preservation for perishable products. *Int. J. Biol. Macromol.* **2023**, *228*, 286–298. [CrossRef]
30. Wichai, S.; Chuysinuan, P.; Chaiarwut, S.; Ekabutr, P.; Supaphol, P. Development of bacterial cellulose/alginate/chitosan composites incorporating copper (II) sulfate as an antibacterial wound dressing. *J. Drug. Deliv. Sci. Tec.* **2019**, *51*, 662–671. [CrossRef]
31. Samadzadeh, M.; Boura, S.H.; Peikari, M.; Kasiriha, S.M.; Ashrafi, A. A review on self-healing coatings based on micro/nanocapsules. *Prog. Org. Coat.* **2010**, *68*, 159–164. [CrossRef]
32. Yan, X.X.; Peng, W.W. Preparation of microcapsules of urea formaldehyde resin coated waterborne coatings and their effect on properties of wood crackle coating. *Coatings* **2020**, *10*, 764. [CrossRef]
33. Yan, X.X.; Peng, W.W.; Qian, X.Y. Effect of water-based acrylic acid microcapsules on the properties of paint film for furniture surface. *Appl. Sci.* **2021**, *11*, 7586. [CrossRef]
34. Garcia, A.; Schlangen, E.; van de Ven, M.; Sierra-Beltran, G. Preparation of capsules containing rejuvenators for their use in asphalt concrete. *J. Hazard. Mater.* **2010**, *184*, 603–611. [CrossRef] [PubMed]
35. *GB/T 11186.3-1989*; Methods for Measuring the Colour of Paint Films. Part III: Calculation of Colour Differences. Standardization Administration of the People's Republic of China: Beijing, China, 1990.
36. *GB/T 9754-2007*; Paints and Varnishes-Determination of Specular Gloss of Non-Metallic Paint Films at 20°, 60° and 85°. Standardization Administration of the People's Republic of China: Beijing, China, 2007.
37. *GB/T 6739-2006*; Paint and Varnishes-Determination of Film Hardness by Pencil Test. Standardization Administration of the People's Republic of China: Beijing, China, 2006.

38. *GB/T 4893.9-2013*; Test of Surface Coatings of Furniture—Part 9: Determination of Resistance to Impact. Standardization Administration of the People's Republic of China: Beijing, China, 2013.
39. *GB/T 4893.4-2013*; Test of Surface Coatings of Furniture—Part 4: Determination of Adhesion-Cross Cut. Standardization Administration of the People's Republic of China: Beijing, China, 2013.
40. *GB/T 21866-2008*; Test Method and Effect for Antibacterial Capability of Paints Film. Standardization Administration of the People's Republic of China: Beijing, China, 2008.
41. *GB 18580-2001*; Indoor Decorating and Refurbishing Materials—Limit of Formal Dehyde Emission of Wood Based Panels and Finishing Products. Standardization Administration of the People's Republic of China: Beijing, China, 2001.
42. Jaroensaensuai, J.; Wongsasulak, S.; Yoovidhya, T.; Devahastin, S.; Rungrassamee, W. Improvement of Moist Heat Resistance of Ascorbic Acid through Encapsulation in Egg Yolk-Chitosan Composite: Application for Production of Highly Nutritious Shrimp Feed Pellets. *Animals* **2022**, *12*, 2384. [CrossRef]
43. Uetsuji, Y.; Fukui, N.; Yagi, T.; Nakamura, Y. The effect of number of chemical bonds on intrinsic adhesive strength of a silane coupling agent with metals: A first-principles study. *J. Mater. Res.* **2022**, *37*, 923–932. [CrossRef]
44. Lai, Y.K.; Tang, Y.X.; Gong, J.J.; Gong, D.G.; Chi, L.F.; Lin, C.J.; Chen, Z. Transparent superhydrophobic/superhydrophilic TiO_2-based coatings for self-cleaning and anti-fogging. *J. Mater. Chem.* **2012**, *22*, 7420–7426. [CrossRef]
45. Yu, Z.H.; Yan, Z.Y.; Zhang, F.H.; Wang, J.X.; Shao, Q.; Murugadoss, V.; Alhadhrami, A.; Mersal, G.A.M.; Ibrahim, M.M.; El-Bahy, Z.M.; et al. Waterborne acrylic resin co-modified by itaconic acid and γ-methacryloxypropyl triisopropoxidesilane for improved mechanical properties, thermal stability, and corrosion resistance. *Prog. Org. Coat.* **2022**, *168*, 106875. [CrossRef]
46. Li, J.H.; Zhuang, S.L. Antibacterial activity of chitosan and its derivatives and their interaction mechanism with bacteria: Current state and perspectives. *Eur. Polym. J.* **2020**, *138*, 109984. [CrossRef]
47. Fan, Q.W.; Fan, X.J.; Fu, P.; Li, Y.; Zhao, Y.X.; Hua, D.L. Anaerobic digestion of wood vinegar wastewater using domesticated sludge: Focusing on the relationship between organic degradation and microbial communities (archaea, bacteria, and fungi). *Bioresour. Technol.* **2022**, *347*, 126384. [CrossRef]
48. Ban, Z.J.; Zhang, J.L.; Li, L.; Luo, Z.S.; Wang, Y.J.; Yuan, Q.P.; Zhou, B.; Liu, H.D. Ginger essential oil-based microencapsulation as an efficient delivery system for the improvement of Jujube (Ziziphus jujuba Mill.) fruit quality. *Food Chem.* **2020**, *306*, 125628. [CrossRef] [PubMed]
49. Rosano, G.L.; Morales, E.S.; Ceccarelli, E.A. New tools for recombinant protein production in *Escherichia coli*: A 5-year update. *Protein Sci.* **2019**, *28*, 1412–1422. [CrossRef] [PubMed]
50. Bayer, A.S.; Schneider, T.; Sahl, H.G. Mechanisms of daptomycin resistance in *Staphylococcus aureus*: Role of the cell membrane and cell wall. *Ann. N. Y. Acad. Sci.* **2013**, *1277*, 139–158. [CrossRef] [PubMed]